A New Method for Blocking Third-Zone Distance Relays During Stable Power Swings

Don Kang, *Student Member, IEEE*, and Ramakrishna Gokaraju, *Senior Member, IEEE*

***Abstract*—The improper operation of the third-zone distance protection has been attributed as one of the factors for power system blackouts. The third-zone protection could incorrectly operate during power-swing scenarios. This research proposes a fast and practical methodology using local measurements for blocking the third-zone distance relays during stable power swings. The proposed scheme is referred to as the BTZ scheme. The proposed method calculates the relative speed of a fictitious equivalent machine from the local relay measurements. If the relative speed goes through a zero crossing, the swing is classified as a stable power swing; whereas if the speed does not go through a zero value, then the swing is classified as an unstable power swing. The benefit of the proposed method is that it analyzes the power swings from a system stability point of view, and does not need rigorous offline simulation studies to determine the relay settings. The performance of the proposed method in this paper is compared with an industry-standard method (conventional double blinder method). As is well known, the settings of the blinder-based methods are system specific and need several simulations to arrive at the blinder values. Transient simulation studies on a three-bus system and a modified Western Coordination Council 9-bus system are used to test the performance of the proposed approach.**

***Index Terms*—Distance relay, outages, power-swing identification, relay algorithm, third-zone blocking.**

I. Introduction

THE distance relay provides protection for the transmission lines connected to a network by measuring the impedance at the relay point, which is proportional to the distance to a fault and is independent of the fault current level [1]. This protection is most commonly used by utilities for transmission line protection because of its simplicity, i.e., it is based on local measurements. The modern trend in "smart grid terms" for applying distance protection is "think globally and act locally."

Power system protective relays are implemented by dividing the power system into protection zones in which the fault can be recognized and be removed by disconnecting a minimum portion of the system [2]. When a fault happens in the transmission system, the primary relay assigned to the zone is supposed to operate. Generally for transmission line distance protection, three protection zones are applied to provide backup for the remote adjacent line section. The Zone 3 distance relay is an overreaching zone providing remote back up protection when the local primary protection or the zone 2 remote backup fails for a local fault. The Zone 3 time delay is typically 1–2 seconds to achieve the coordination [3]. The infeeds and outfeeds at the remote bus result in Zone 3 underreaching or overreaching. Distance relays may also operate falsely during transient stability conditions (i.e., due to power swing phenomenon) and voltage instability conditions. The long reach of the distance relays even though useful from the system security point of view may conflict with the line load ability requirements.

Undesired Zone 3 tripping has been attributed as one of the factors for large power system outages [3]–[5]. Stable power swing conditions, which are not detrimental to the power system, sometimes intrude into the Zone 3 region of the distance relays and cause mal operation. The standard power swing detection methods and relay blocking requires detailed time-domain stability studies on the system for various contingency conditions. The correct operation of remote protective relays (Zone 3 operation) is very important so that a large section of the power system does not fail unnecessarily.

Detecting stable power swings and blocking is critical for distance relay's proper operation. The traditional power swing detection blinder scheme detects the difference of the rate of change of the positive-sequence impedance vector [6]. It uses the concept that during a power swing that it takes more time for the machine rotor angle to change due to its large inertia and also for the change of the apparent impedance measured at a distance relay during the power swing condition. On the contrary, during a faulted condition the rate of change of the apparent impedance is almost immediate. The blinder scheme is practical, although finding the settings for blocking during stable power swing and tripping during unstable power swings of the distance relay is not an easy task. It requires detailed stability studies on the system for various contingency conditions. For example, the fastest rate of a possible power swing has to be decided based on large number of stability studies. It is very difficult to find all the power swing scenarios and operating conditions on a large power system [6]. Moreover, the best location to block the power swing or to separate the faulted portion of the power system also requires numerous stability studies [7]. There are a few other reported schemes similar to the blinder scheme: the rate of change of impedance based method [6] and a rate of change of resistance based method [8].

Repositioning the distance characteristic is one mechanism to improve the distance relay's operation during heavy loads and power swings. The angle adjustment of Mho characteristics is reported in [3]. The alteration increases the maximum sensitivity angle to optimize the resistive coverage for a stable power swing. Other alternate schemes include changing the zone shape of

Manuscript received July 02, 2015; revised December 02, 2015; accepted January 16, 2016. Date of publication January 21, 2016; date of current version July 21, 2016. Paper no. TPWRD-00862-2015.

The authors are with the Electrical and Computer Engineering Department, University of Saskatchewan, Saskatoon, SK S7N 5A9 Canada (e-mail: rama.krishna@usask.ca; dok524@mail.usask.ca).

Color versions of one or more of the figures in this paper are available online at http//ieeexplore.ieee.org.

Digital Object Identifier 10.1109/TPWRD.2016.2520394

the distance relay, supervised zone tripping scheme, studying load encroachment characteristics, etc. [3]. All these methods could be categorized as changing of the zone characteristics schemes as well. However, similar to original blinder methods, the shortcoming of the above alternate schemes is that the loci of the possible power swing have to be found based on extensive stability studies and not all power swing scenarios and operating conditions could be covered.

Benmouyal *et al.* [9] proposed a swing-center voltage (SCV) method, which detects the rate of change of the swing-center voltage of a power system to determine whether it is a stable power swing or an unstable condition. The swing-center voltage method is independent of the system source impedance and the line impedance, and its magnitude is equal to the angle difference of sources, and is bounded to 0 to 1 per unit [9]. The scheme is applicable for a two-source equivalent system. There is no literature discussing the SCV method for larger power system networks.

Pattern recognition methods have also been applied for power swing identification. A Wavelet Transform was discussed by Brahma in 2007 [10]. A Support Vector Machine (SVM) based power swing identification scheme was proposed by Seethalekshmi K., *et al.* in 2010 [11]. A Zone 3 blocking scheme using a polynomial curve fitting approach was discussed by Sriram *et al.* in 2014 [12], and a Zone 3 protection method using transient monitoring function was discussed by Nayak *et al.* in 2015 [13], etc. Pattern recognition approaches require training using several offline simulation runs. Polynomial curve fitting approaches may be difficult to apply when the system is at a boundary of instability conditions.

The objective of this research/paper is to develop a reliable power swing detection scheme that can identify whether it is a stable or unstable power swing encroaching into Zone 3 by employing a First Zero Crossing (FZC) concept. It can block the third zone (BTZ) protection during stable power swings, in order to prevent unnecessary tripping of distance relays and maintain power supply continuity. The proposed power swing identification algorithm for Zone 3 distance relays blocking is simple, involves only a few calculation steps, and can be applied to any power system configuration. The main novelty of this technique is that it does not require a priori stability studies to find relay settings unlike the conventional blinder based technique. The input measurements to this relay are basic electrical quantities which could be easily measured locally on any transmission line.

Simulation studies have been carried out on a simple 3-bus system and a modified Western Systems Coordinating Council (WSCC) 9-bus system [14] using the PSAT software [15].

The paper is organized as follows: Section II discusses how the single machine infinite bus equivalent is obtained from the local measurements at a relay location. A small three bus example is used to demonstrate the proposed methodology for identifying whether the swing is a stable or an unstable swing. Sections III gives the simulation results using the modified WSCC 9-bus test system. Section IV is the proposed BZT scheme and traditional Blinder method comparison. Section V gives the final conclusions and the contributions of this paper.

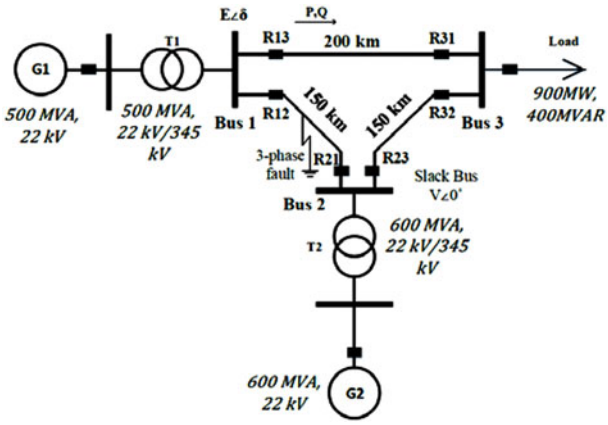

Fig. 1. A 3-bus, 345 kV test system example.

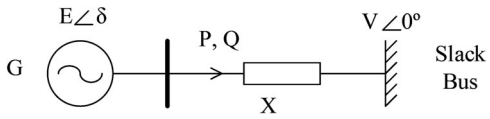

Fig. 2. Equivalent single machine infinite bus representation of the 3-bus test system example.

II. Proposed Methodology

A small 345 kV test system example shown in Fig. 1 is used for the purpose of explaining the proposed algorithm. It consists of two generators and a load bus (3-bus power system). The system parameters are given in Table IV. The equations for the proposed method are developed using the local measurements at the relay location R13 and the power-angle characteristics equations. The transient stability of the system is analyzed using the classical swing equation. The program is developed to include a base case power flow to initialize the simulations and a three-part code for pre-fault, during fault, and post fault calculations. A three phase fault is applied on line 1–2 at 1/3 of the distance from bus 1 to bus 2 to explain the proposed approach for R13.

At the relay location R13, the entire test system can be represented with a single machine infinite bus (SMIB) equivalent system as shown in Fig. 2 [16]–[18]. The two unknown parameters in the SMIB system are the voltage angle δ at R13 and the equivalent reactance X of the equivalent SMIB system. The following description explains how these two quantities are determined.

The SMIB in this paper is obtained in an online fashion as shown in Fig. 2 using only the local measurements and does not involve the inertia term. The active power, reactive power, bus voltage $P, Q, E\angle\delta$ for the SMIB system in Fig. 2 are same as the $P, Q, E\angle\delta$ measured at Bus 1 for distance relay R13.

The phase one of the proposed algorithm is determining the equivalent reactance X of the equivalent SMIB system.

The power flow in the SMIB equivalent system is given by,

$$P = \frac{EV}{X}\sin\delta \tag{1}$$

$$Q = \frac{E^2}{X} - \frac{EV}{X}\cos\delta \tag{2}$$

where P is the active power, Q is the reactive power, E is the Bus 1 voltage magnitude, V is Bus 2 voltage magnitude, X is the equivalent reactance, δ is the angle difference between Bus 1 and Bus 2 as shown in Fig. 1.

Eliminating δ in (1) and (2),

$$\left(\frac{PX}{EV}\right)^2 + \left(\frac{E^2 - QX}{EV}\right)^2 = 1 \tag{3}$$

The fictitious reactance X can be obtained by solving the derived (4).

$$\left(P^2 + Q^2\right) X^2 - 2E^2 QX + E^4 - E^2 V^2 = 0 \tag{4}$$

With the calculated X, the phase two of the algorithm is calculating the speed of the fictitious synchronous machine shown in Fig. 2 during a power swing. The fictitious machine speed equation as the following is also derived from above power angle equations (1) and (2). Differentiating (1),

$$\frac{dP}{dt} = \left(\frac{EV}{X}\right)\cos\delta\left(\frac{d\delta}{dt}\right) \tag{5}$$

Since $\frac{d\delta}{dt} = \omega r$ and $\cos\delta$ can be obtained from (2),

$$\frac{dP}{dt} = \left(\frac{E^2 - QX}{X}\right)\omega r \tag{6}$$

$$\omega r = \left(\frac{dP}{dt}\right) \Big/ \left(\frac{E^2 - QX}{X}\right) \tag{7}$$

where ωr is the fictitious synchronous machine relative speed.

Thus, the frequency of the system or the speed of the equivalent synchronous machine can be obtained as long as $\frac{dP}{dt}$ is known by the following digital simulation.

$$\frac{dP}{dt} \approx \frac{\Delta P}{\Delta t} = \frac{P_t - P_{t-1}}{\Delta t} \tag{8}$$

Substituting (8) into (7),

$$\omega r = \frac{\left(\frac{P_t - P_{t-1}}{\Delta t}\right)}{\left(\frac{E^2 - QX}{X}\right)} \tag{9}$$

The time step Δt in the simulation is generally constant and is considered to be a small value. When the variable ω is the actual rotor speed of the equivalent machine, and the relative speed ω_r is thus given by

$$\omega_r = \omega - \omega_s \tag{10}$$

$$\omega_s = 2\pi f_s \tag{11}$$

where ω_s is synchronous speed, f_s is synchronous frequency.

A stable swing is distinguished from an unstable one from the fact that the speed ω of the machine G in SMIB system in Fig. 2 reaches a synchronous value called First Zero Crossing (FZC) in this research, before the machine starts accelerating again. In the case of an unstable swing, the machine G starts accelerating before the relative speed becomes zero or the speed becomes synchronous. The stable or unstable swing identification with the relative speed $\omega_r = \omega - \omega_s$ is graphically illustrated in Fig. 3. Fig. 4 demonstrates the stable and unstable swings shown in Fig. 3 from the physics point of view (using the equilibrium

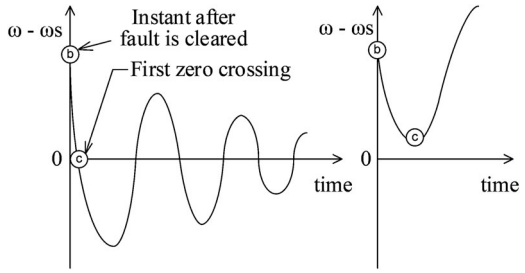

Fig. 3. Relative speed of the equivalent machine due to a stable and unstable power swing.

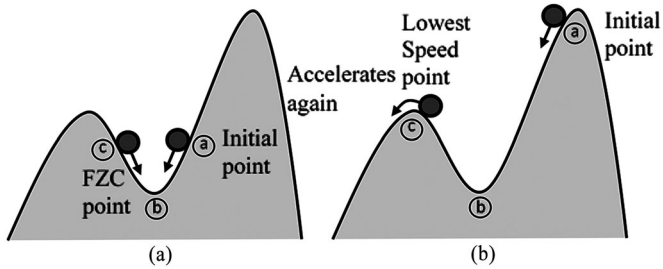

Fig. 4. Stable, unstable equilibrium points for power swings shown in Fig. 3.

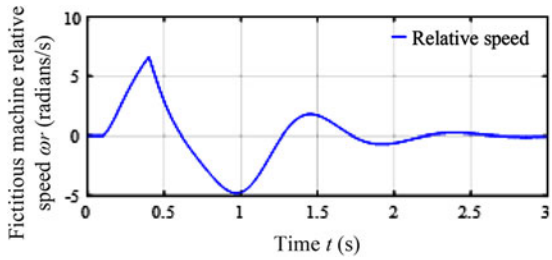

Fig. 5. Relative speed of the generator calculated from measurements at R13.

points). The point 'a' corresponds to the instant fault happens (i.e., relative speed is zero), point 'b' corresponds to the instant fault is cleared (when the speed is at its maximum value), point 'c' corresponds to zero crossing point (for a stable swing) or the lowest speed point (for an unstable swing).

Fig. 5 shows the results (calculated speed with measurements at R13) when a three-phase fault of fault duration equal to 0.40 seconds is applied on line 1–2 at 1/3 of the distance between bus 1 to bus 2. The fault is applied at 0.1 s. The first zero crossing is detected at 0.61 s indicating a stable power swing. In the case of an unstable swing, the machine G's relative speed goes to a minimum point (does not cross the zero point) before it starts accelerating again. Fig. 6 shows the results for an unstable swing with a fault duration of 0.45 seconds. The critical fault clearing time is found to be 0.44 seconds for these studies.

In summary, for a fault occurring in power system, the nature of power swing (post-fault) can be evaluated within the line distance relay module using the proposed algorithm to decide whether to block the Zone 3 or not. If it is a stable power swing, the zone 3 could be blocked irrespective of whether it encroaches into Zone 3 or not, it need not trip the breaker

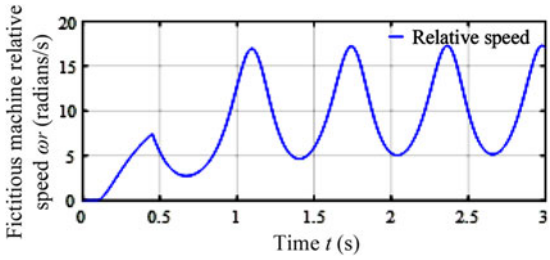

Fig. 6. Relative speed of the generator calculated from measurements at R13.

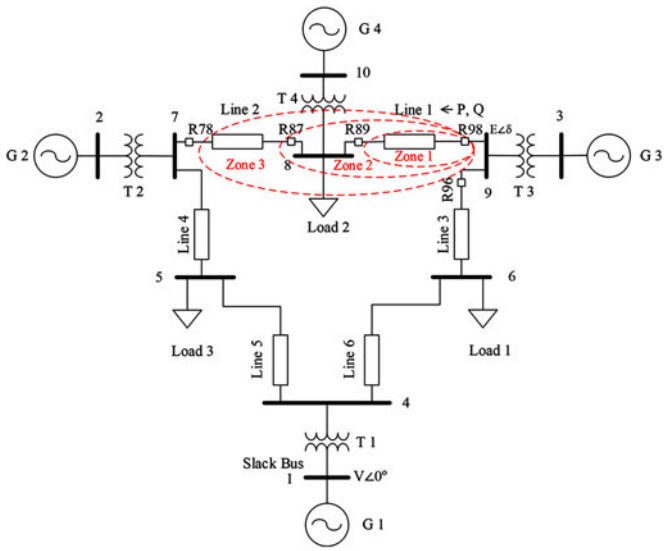

Fig. 7. WSCC 9-bus system modified with infeed generator G 4. [14].

using this arrangement. If the FZC or unstable swing could be detected much before the encroachment, the proposed scheme will be very useful for real applications.

III. Simulation Studies

A. Test System

The proposed BTZ scheme has been tested on a modified WSCC 9-bus system shown in Fig. 7. One 250 MVA additional generator G 4 has been connected to load Bus 8 of the original WSCC 9-bus system [14] to simulate scenarios where the impedance loci enters into Zone 3 of the distance relay. The system parameters are given in Table V.

In order to simulate the power swing encroaching into the Zone 3 of the relay, three phase to ground faults are applied at different locations in the system. A numerical optimization procedure (Laguerre method) is used to solve the polynomial (4) and calculate the reactance X of the fictitious system. The value X and the rate of change of active power $\left(\frac{dP}{dt}\right)$ is utilized to find the relative speed ω_r of the equivalent synchronous machine shown in Figs. 8, 10 and 12. The apparent impedances measured at the relay location R98 and R78, and their loci, and Zone 3 characteristics are shown in Figs. 9, 11, and 13.

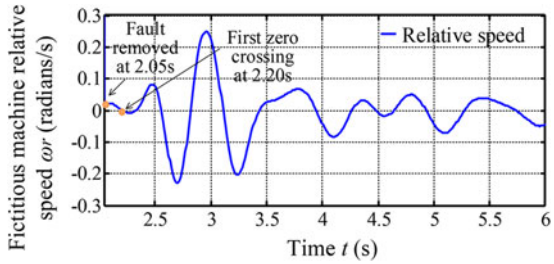

Fig. 8. Fictitious synchronous machine relative speed for study case 1 on distance relay R98.

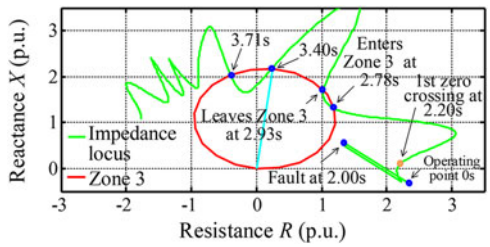

Fig. 9. Impedance locus measured at distance mho relay R98 on Zone 3 characteristics for study case 1.

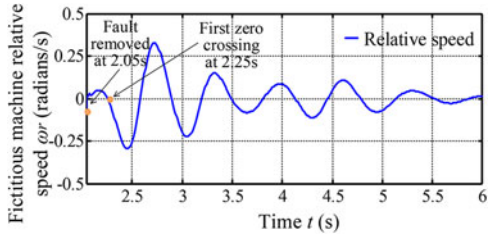

Fig. 10. Fictitious synchronous machine relative speed for study case 2 on distance relay R98.

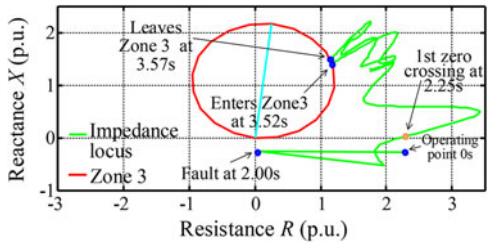

Fig. 11. Impedance locus measured at distance mho relay R98 on Zone 3 characteristics for study case 2.

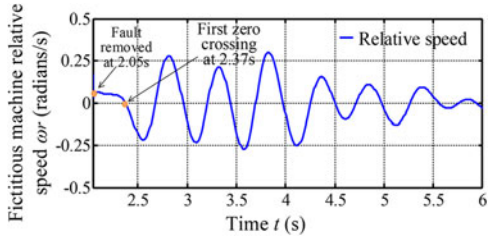

Fig. 12. Fictitious synchronous machine relative speed for study case 1 on distance relay R78.

TABLE I
SUMMARY OF STABLE POWER SWING STUDIES ON DISTANCE RELAY R98 IN MODIFIED WSCC SYSTEM

Case No.	1	2	3	4	5	6
Fault Location Bus No.	7	6	8	8	5	8
Fault in Protection Zones (Y/N)	N	N	Y	Y	N	Y
Fault Duration (cycle)	3	3	3	6	3	9
Fault Duration (s)	0.05	0.05	0.05	0.10	0.05	0.15
FZC After Fault Removal (s)	0.15	0.20	0.24	0.25	0.18	0.33
First Zone 3 Entering (s)	0.73	1.47	0.58	0.48	1.38	0.52
Relay Reaction Time After FZC (cycle)	35	76	20	14	72	11
Zone 3 Blocking Decision (Y/N)	Y	Y	Y	Y	Y	Y

B. Studies for Distance Relay R98

The distance relay R98 is located at the sending end of transmission Line 1 at bus 9. Three protection zones of R98 are shown in Fig. 7. Zone 3 here covers Line 1 plus 120% of Line 2. Transmission Line 2 distance relay R87 at Bus 8 is backed up by R98.

In the first case study (Case 1) of R98, the fault is applied at 2.00 s and removed at 2.05 s at Bus 7. The fault duration (0.05 s is less than the time delay setting for Zone 3, i.e., 1.5 s (90 cycles). For this case study, the primary protection is at R87 (i.e., Zone 1). It can be seen from Fig. 8 that the fictitious machine speed ω reaches the synchronous value at 2.20 s (the relative speed is going to be zero), i.e., 0.15 s after the fault is removed. The trace of the impedance locus change is shown in Fig. 9. The first time the locus enters Zone 3 is at 2.78 s (i.e., 35 cycles after the FZC). So there is adequate room for blocking the third zone.

For Case 2, the fault is applied at Bus 6, which is outside the reach of Zone 3 of the distance relay R98. The primary distance relay R96 is assumed to fail to respond to the fault. Fig. 10 shows the plot of the relative speed of the equivalent machine. Fig. 11 gives the plot of the impedance locus. The first zero crossing is obtained at 2.25 s; whereas the instant at which the impedance locus enters the Zone 3 is at 3.52 s (or 76 cycles after the FZC, on the impedance locus in Fig. 11). Thus it gives sufficient time to block the third zone of the relay R98.

Similar type of studies were done for R98 when the fault is applied at other locations in the system (buses 5 and 8). The proposed BZT scheme was also tested for different fault duration values (i.e., when fault applied at bus 8 is 0.05 s, 0.10 s and 0.15 s, respectively). Similar to Cases 1 and 2, the results here show that FZC can be detected much before the time the impedance locus enters Zone 3. So for all cases there is sufficient time for blocking Zone 3 for R98. The results are summarized in Table I (the additional cases are listed from 3–6 respectively).

C. Studies for Distance Relay R78

The distance relay R78 is located at the sending end of transmission Line 1 at bus 7. The protection zones of R78 are not drawn in Fig. 7 for clarity, Its protection Zone 3 covers Line 2 plus 120% of Line 1. The distance relay R89 at Bus 8 is backed up by R78.

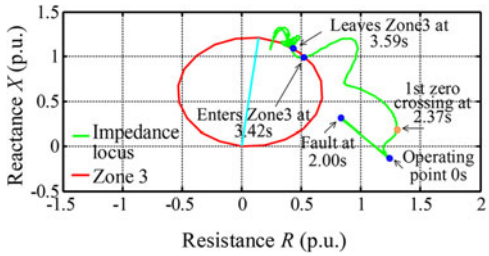

Fig. 13. Impedance locus measured at distance mho relay R78 on Zone 3 characteristics for study case 1.

TABLE II
SUMMARY OF STABLE POWER SWING STUDIES ON DISTANCE RELAY R78 IN MODIFIED WSCC SYSTEM

Case No.	1	2	3	4	5
Fault Location Bus No.	9	6	8	8	5
Fault in Protection Zones (Y/N)	N	N	Y	Y	N
Fault Duration (cycle)	3	3	3	6	6
Fault Duration (s)	0.05	0.05	0.05	0.10	0.10
FZC After Fault Removal (s)	0.32	0.23	0.17	0.18	0.20
First Zone 3 Entering (s)	1.37	NA	0.63	0.57	0.56
Relay Reaction Time After FZC (cycle)	73	NA	28	23	22
Zone 3 Blocking Decision (Y/N)	Y	N	Y	Y	Y

For case study (Case 1 of R78), the fault is applied at 2.00 s and removed at 2.05 s at Bus 9. The relay R89 is assumed to not operate for this case study. The relative speed of the equivalent machine reaches a zero value at 2.37 s (see Fig. 12), i.e., 0.32 s after the fault is removed. The plot of the impedance locus is shown in Fig. 13. The impedance locus enters Zone 3 at 3.59 s, i.e., 73 cycles after the FZC. So again in this case it can be seen that there is sufficient time for blocking Zone 3 during a stable power swing.

Four more studies are reported for R78 with the faults applied at different locations in the system buses 5, 6 and 8. The effectiveness of BZT scheme for different three phase fault durations are also examined (fault durations of 0.05 s and 0.10 s at bus 8). The results show that the FZC can be detected much before the impedance locus enters Zone 3. The study case results are summarized in Table II and the additional cases are shown from 2–5.

D. Discussion of the Results

The simulation studies are done using the PSAT software and the proposed algorithm has been developed in FORTRAN. Since the studies are done in an offline fashion, the computation times are compared as a percentage. The algorithm took only about 6% of the time step used for the measurements for the distance relay. Thus, the computation time requirement of the proposed algorithm is fast enough for a real-time application.

In all simulation cases, the first zero crossing is obtained much earlier (less than 0.33 s) than the impedance trajectory enters in Zone 3, so the Zone 3 could be blocked.

Moreover, the basic difference between balanced three phase fault and power swing is the rate of change of measured

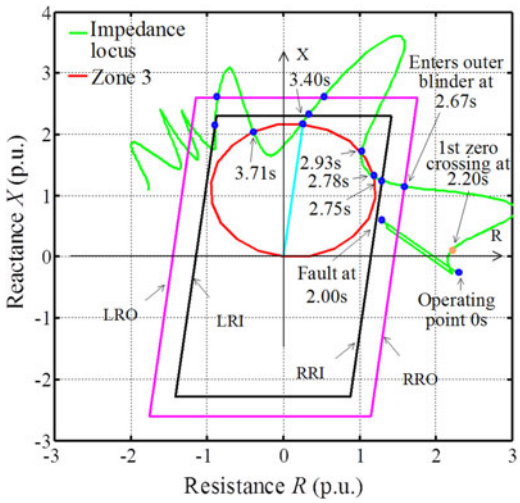

Fig. 14. BZT and Blinder scheme comparison for study case 1 on relay R98.

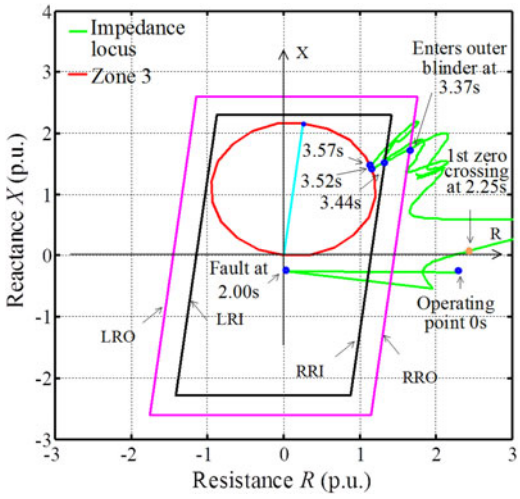

Fig. 15. BZT and Blinder scheme comparison for study case 2 on relay R98.

impedance. From the simulation results presented in the paper, the impedance locus at fault moves instantaneously, whereas the ones of power swings move at a much slower rate. The blocked distance relay should be unblocked to clear fault when fault is detected during a power swing.

IV. Comparison to Traditional Scheme

A. Blinder Scheme Settings

The effectiveness of the developed BZT scheme has been verified by comparing it to the conventional power swing identification and blocking blinder based schemes. A two concentric polygons blinders are established inclined at the transmission line angle, i.e., 81°, in the power swing studies for distance relay R98 as shown in Figs. 14 and 15.

The blinder settings described in [6] and [19] are used for the test system. The inner blinder is placed outside the protection Zone 3 characteristics. The outer blinder settings are considered to keep 5% security margin resistively away from the possible maximum load, and 20% margin reactively away from the maximum mho relay reach. The settings are given below.

Right Resistance Inner (RRI): 1.1451 p.u.

Right Resistance Outer (RRO): 1.4506 p.u.

Left Resistance Inner (LRI): -1.1451 p.u.

Left Resistance Outer (LRO): -1.4506 p.u.

The maximum slip frequency is about 2 Hz. The minimum block duration timer setting is 0.65 cycles, which is equal to 11 ms. [19]

TABLE III
Summary of BZT and Blinder Scheme Comparison on Distance Relay R98 in Modified WSCC System

Case No.	1	2	3	4
Fault Location Bus No.	7	6	8	8
Fault in Protection Zones (Y/N)	N	N	Y	Y
Fault Duration (s)	0.05	0.05	0.05	0.10
FZC After Fault Removal (s)	0.15	0.20	0.24	0.25
First Outer Blinder Entering (s)	0.62	1.32	0.51	0.45
Zone 3 Blocking Decision (Y/N)	Y	Y	Y	Y
Swing Entering Outer Blinder (s)	Y	Y	Y	Y
Swing Entering Inner Blinder (Y/N)	Y	Y	Y	Y

TABLE IV
System Parameters for Two Machine System

Base MVA	100	
Base kV	345	
	Generator	
No.	G1	G2
Rated MVA	500	600
x'_d (pu)	0.23	0.23
	Transf.	
No.	T1	T2
kV	22/345	22/345
x_T (pu)	0.12	0.12

B. BZT and Blinder Scheme Comparison

For case 1 studies for distance relay R98, the impedance locus enters the outer blinder when fault happens at 2.00 s. Since for a fault, the rate of change of impedance is instantaneous, the blinders settings would not classify it as a swing trajectory during the fault duration. Once the fault is removed, the swing impedance locus enters the outer blinder enters at 2.67 s, and then enters into inner blinder as well, and will be identified incorrectly as an out-of-step phenomenon by the conventional two blinder scheme. The proposed BZT scheme correctly identifies it as a stable power swing as shown in the results in Fig. 8. In Fig. 14, it can be seen that the impedance locus reenters the outer and the inner blinders from the top so the blinder based technique is prone to incorrect operation.

For case 2 for R98, the fault is again applied at 2.00 s. The impedance locus during the short fault duration of 0.05 s would not be obviously picked up by the blinders. Similar to the Case 1

TABLE V
SYSTEM PARAMETERS FOR MODIFIED WSCC SYSTEM

Base MVA	100			
Base kV	230			
		Generator		
No.	1	2	3	4
Rated MVA	60.5	60.0	60.0	250.0
Voltage (kV)	16.5	18.0	13.8	13.8
Type	hydro	steam	steam	steam
Speed (r/min)	1800	3600	3600	3600
x_d (pu)	0.1460	0.8958	1.3125	1.3125
x'_d (pu)	0.0608	0.1198	0.1813	0.1813
x_q (pu)	0.0969	0.8645	1.2578	1.2578
x'_q (pu)	0.0969	0.1969	0.25	0.25
x_l (pu) (leakage)	0.0336	0.0521	0.0742	0.0742
$r'_{d\,0}$ (pu)	8.96	6.00	5.89	5.89
$r'_{q\,0}$ (pu)	0	0.535	0.600	0.600
		Transf.		
No.	1	2	3	4
kV	16.5/230	18/230	13.8/230	13.8/230
x_T (pu)	0.576	0.0625	0.0586	0.0586

studies, the impedance locus for a stable swing (see the relative speed trajectory in Fig. 10) will enter into the inner blinder of the double blinder scheme and would result in an incorrect classification (as an unstable swing).

Similar results are also observed in the other two case studies for R98 when the fault is applied on bus 8 with 0.05 s and 0.10 s fault durations. The primary benefit of the proposed method in the paper is that it can detect stable power swings correctly and faster than the conventional type two blinder scheme. The four comparison case results are summarized in Table III.

V. CONCLUSION

In this paper a third-zone blocking method for stable power swing has been proposed. A SMIB equivalenting procedure is described using the local measurements of voltage, active and reactive power. Once the SMIB is obtained in an online fashion, the relative speed of the equivalent machine could be analyzed with respect to time to identify whether it is a stable power swing or not (by looking at the zero crossing). The scheme has been tested on a simple 3-bus system and a modified WSCC 9-bus test system. It is shown to be effective compared to the conventional double blinder based scheme.

The proposed BTZ scheme could correctly identify stable power swings. The proposed method is general, does not involve any parameter settings beforehand. The primary advantage of the proposed method is that it is local measurement based.

ACKNOWLEDGMENT

The authors would like to thank Prof. M. Ramamoorty (Retired Director General Central Power Research Institute, Bangalore, India), S. Raman (Visiting Student, University of Saskatchewan, Saskatoon, SK, Canada), and Dr. E. Pajuelo (University of Saskatchewan, Saskatoon, SK, Canada) for discussing the proposed methodology during development.

REFERENCES

[1] S. H. Horowitz and A. G. Phadke, "Nonpilot distance protection of transmission lines," *Power System Relaying* 3rd, Hoboken, NJ, USA: Wiley, 2008.
[2] W. A. Elmore, "Line and circuit protection," *Protective Relaying Theory and Applications*, New York, USA: Marcel Dekker, 2004.
[3] IEEE PSRC Working Group D4, "Application of overreaching distance relays," 2009.
[4] S. H. Horowitz and A. G. Phadke, "Third zone revisited," *IEEE Trans. Power Del.*, vol. 21, no. 1, pp. 23–29, Jan. 2006.
[5] North American Electric Reliability Council, *"August 14, 2003 blackout: NERC actions to prevent and mitigate the impacts of future cascading blackouts,"* Princeton, NJ, USA, Feb. 10 2004.
[6] M. McDonald *et al.*, IEEE PSRC Working Group D6, "Power swing and out-of-step considerations on transmission lines," Jun. 2005.
[7] *ANSI/IEEE C37.90 IEEE Standard for Relays and Relay Systems Associated With Electric Power Apparatus* ANSI/IEEE C37.90, 1989.
[8] Z. D. Gao and G. B. Wang, "A new power swing block in distance protection based on a microcomputer principle and performance analysis," in *Proc. Int. Conf. Adv. Power Syst. Control Oper. Manage.*, 1991, pp. 623–628.
[9] G. Benmouyal, D. Tziouvaras, and D. Hou, "Zero-setting power-swing blocking proctection," *31st Annu. Western Protect. Relay Conf.*, Spokane, WA, USA, Oct. 19–21 2004.
[10] S. M. Brahma, "Distance relay with out-of-step blocking function using wavelet transform," *IEEE Trans. Power Del.*, vol. 22, no. 3, pp. 1360–1366, Jul. 2007.
[11] K. Seethalekshmi, S. N. Singh, and S. C. Srivastava, "SVM based power swing identification scheme for distance relays," in *Proc. IEEE Power Energy Soc. Gen. Meeting*, 2010, pp. 1–8.
[12] C. Sriram, D. R. Kumar, and G. S. Raju, "Blocking the distance relay operation in third zone during power swing using polynomial curve fitting method," in *Proc. Int. Conf. Smart Elect. Grid*, 2014, pp. 1–7.
[13] P. K. Nayak, A. K. Pradham, and P. Bajpai, "Secured zone 3 protection during stressed condition," *IEEE Trans. Power Del.*, vol. 30, no. 1, pp. 89–96, Feb. 2015.
[14] P. M. Anderson and A. A. Fouad, "Classical stability study of a 9-bus system," *Power System Control and Stability* 2nd, Hoboken, NJ, USA: Wiley, 2004.
[15] F. Milano, *Power System Analysis Toolbox*, Feb. 14 2008 Documentation for PSAT version 2. 0. 0.
[16] Y. Xue, T. Van Custem, and M. Ribbens-Ravella, "Extended equal area criterion justifications, generalizations, applications," *IEEE Trans. Power Syst.*, vol. 4, no. 1, pp. 44–52, Feb. 1989.
[17] L. Neerugattu and G. S. Raju, "New criteria for voltage stability evaluation in interconnected power system," *Nat. Power Syst. Conf.*, Varanasi, India, Dec. 12–14 2012.
[18] B. Shrestha, R. Gokaraju, and M. Sachdev, "Out-of-step protection using state-plane trajectories analysis," *IEEE Trans. Power Del.*, vol. 28, no. 2, pp. 1083–1093, Apr. 2013.
[19] F. Plumpire, S. Brettschneider, A. Hiebert, M. Thompson, and M. Mynam, BC Hydro Cegertec, BC Transmission Corporation, Schweitzer Engineering Laboratories, Inc., *"Validation of out-of-step protection with a real time digital simulator,"* 2006.

Don Kang (S'16) received the M.Sc. degree in mechatronics from the University of Saskatchewan, Saskatoon, SK, Canada, in 2008.

He was an Electrical Engineer with Beijing Construction Engineering Group Corp., Beijing, China, from 1990 to 1996; Keyuan Mechanical and Electrical Engineering Company from 1996 to 1998; and Beijing Institute of New Technology Application from 1998 to 2003. He has been an Electrical Engineer with March Consulting Associates Inc., Saskatoon, and is currently undertaking graduate study in the area of transient analysis in power system zone protection in the Electrical and Computer Engineering Department at the University of Saskatchewan.

Ramakrishna Gokaraju (S'88–M'00–SM'15) received the M.Sc. and Ph.D. degrees in electrical and computer engineering from the University of Calgary, Calgary, AB, Canada, in 1996 and 2000, respectively.

He joined the Department of Electrical and Computer Engineering at the University of Saskatchewan, Saskatoon, SK, Canada, as an Assistant Professor in 2003, received tenure/Associate Professorship in 2009, and became a Professor in 2015. During 1992–1994, he was a Graduate Engineer with Larsen & Toubro-ECC, Chennai, India; a Research Engineer with Regional Engineering College, Rourkela, India; and a Project Associate with the Indian Institute of Technology, Kanpur, India. From 1999 to 2002, he was a Research Scientist with the Alberta Research Council and a Staff Software Engineer with the IBM Toronto Laboratory, Toronto, ON, Canada. His current research works are in wide-area-based power systems protection and control, renewable energy integrated systems, and real-time simulations approaches.